Clinical and Experimental Pharmacology and Physiology

WILEY

CEPP Clinical and Experimental Pharmacology and Physiology

ORIGINAL ARTICLE OPEN ACCESS

Exploring Phytochemical Adjuvant Therapy in Melanoma Treatment: The Effects of MAZ-51 and Zingerone on Melanoma Cell Proliferation

Kganya Letsoalo | Charlise Basson | Trevor Nyakudya | Yvette Hlophe

Department of Physiology, School of Medicine, Faculty of Health Sciences, University of Pretoria, Pretoria, South Africa

Correspondence: Yvette Hlophe (yvette.hlophe@up.ac.za)

Received: 23 March 2025 | **Revised:** 11 June 2025 | **Accepted:** 8 July 2025

Funding: This work was supported by the National Research Foundation (NRF) of South Africa (N1F580 A1F685) and the University of Pretoria's postgraduate funding scheme.

Keywords: MAZ-51 and chemotherapeutics | melanoma | phytochemicals | zingerone

ABSTRACT

Current melanoma treatment results in adverse effects, prompting the use of phytochemicals as adjuvant therapy to reduce the reliance on synthetic drugs and combat drug resistance. This study investigated the in vitro effect of (3-(4-Dimethylamino-naphthelen-1-ylmethylene)-1, 3-hydroindol-2-one) (MAZ-51) and zingerone, a ginger derivative, on melanoma cell proliferation in B16-F10 melanoma and HaCaT human keratinocyte cell lines. The cells were treated with MAZ-51 (0.002–0.005 mg/mL) and zingerone (0.5–2 mg/mL) at 24, 48 and 72 h, as well as combined treatment (at IC_{50} at 48 and 72 h), to determine cell numbers using a crystal violet assay, which was also utilised to investigate the effects of vascular endothelial growth factor (VEGF) co-treated medium on cell numbers. Morphological changes were examined using haematoxylin and eosin (H&E) staining and polarisation optical density inferential contrast (PlasDIC) and cell cycle progression using flow cytometry. The B16-F10 half maximal inhibitory concentrations (IC_{50}) were 0.05428, 0.03162 and 0.01204 mg/mL for MAZ-51 at 24, 48 and 72 h, respectively, and 27.9, 2.199 and 1.219 mg/mL for zingerone at 24, 48 and 72 h respectively. Both compounds reduced cell numbers at 48 and 72 h ($p < 0.05$) and co-treatment with VEGF exhibited a decrease in cell numbers. Morphological analysis revealed characteristics of cell death, and flow cytometry analysis exhibited a mitotic block. Our findings demonstrate that individual treatment exhibited significant antiproliferative effects on melanoma cells. However, the combination treatment resulted in a combination index (CI) that is greater than one at IC_{50} and IC_{25}, indicating antagonism. Therefore, future studies should consider the individual effects of the compounds on melanoma proliferation.

1 | Introduction

Cancer initiation and progression is a multifaceted process that transforms normal cells into malignant cells [1]. According to the International Agency for Research on Cancer (IARC), more than 18.1 million new cases and 9.5 million cancer-related deaths were recorded in 2020 [2]. In addition, the IARC estimates that an additional 29.5 million new cases and 16.4 million cancer-related deaths will be recorded by 2040 [2]. South Africa recorded approximately 108 168 new cases and 56 802 cancer-related deaths in 2020. Prostate, lung, colon-rectum cancer, and Kaposi sarcoma are the most prevalent types of cancers among South African males, whereas breast, cervical-uterine, colorectum, and lung cancers are prominent in South African females [2]. Melanoma, an aggressive form of skin cancer, is derived from the neoplastic transformation of melanocytes and is classified into four subgroups, namely: superficial spreading, nodular, lentigo, and

acral lentiginous melanoma [3]. Despite accounting for less than 1% of skin cancer cases, melanoma is responsible for 90% of skin cancer-related deaths due to its high metastatic potential [3].

In contrast to normal cells, which respond to exogenous stimuli to regulate growth and metastasis, tumour cells, through the accumulation of genetic mutations, become insensitive to these anti-mitogenic signals, allowing them to evade the apoptotic and repair mechanisms [4]. To establish a metastatic niche, tumour cells, along with tumour-associated macrophages (TAMs) and stromal cells, secrete various regulatory factors such as growth factors, cytokines, and chemokines that promote a favourable environment for melanoma growth by stimulating the proliferation of lymphatic endothelial cells (LECs), prompting lymphangiogenesis [3, 5]. Lymphangiogenesis, the sprouting of lymphatic vasculature from pre-existing vessels, is primarily driven by vascular endothelial growth factor receptor 3 (VEGFR-3) and its ligands (VEGF-C and D) [5, 6]. Activation of the VEGFR-3 signalling pathway stimulates LEC proliferation and lymphatic vessel remodelling, creating a metastatic route to lymph nodes and secondary locations. The elevated expression of the VEGFR-3/VEGF-C axis is a key prognostic factor in multiple cancers, including melanoma, colorectal, lung adenocarcinoma, and breast cancer [3]. Therefore, targeting this signalling pathway is a potential therapeutic approach for melanoma growth and progression.

Inhibiting the VEGFR-3 pathway by disrupting the binding of VEGF-C/D to their receptor may combat lymphangiogenic metastasis and proliferation [5]. (3-(4-dimethylaminonaphthelen-1-ylmethylene)-1,3-dihydroindol-2-one) MAZ-51, an indolinone-based synthetic molecule, prevents receptor tyrosine kinase (RTK) activity of VEGFR-3 [3, 7]. By hindering VEGF-C induced activation of VEGFR-3, MAZ-51 impedes receptor phosphorylation and activation of downstream signalling pathways and thus inhibits lymphangiogenesis and proliferation [3].

A significant challenge in modern cancer treatment strategies is the development of unintended side-effects due to traditional cancer drugs, which are cytotoxic to both cancerous and non-cancerous cells, leading to common side-effects such as alopecia, neutropenia, neurological disorders, vomiting, nausea, and increased susceptibility to secondary infections [8, 9]. Additionally, combination therapy often involves using multiple chemotherapeutic agents to target different signalling pathways. However, this approach can lead to multidrug resistance, potentially promoting tumour growth and proliferation [3]. Additionally, metabolites of anti-cancer drugs are excreted in wastewater systems, posing an environmental burden [3].

Given the challenges associated with the use of pharmacological agents in the management of cancer, there is a need to align effective cancer treatment with environmental sustainability by exploring alternative treatment strategies. In light of the accumulating evidence against the use of synthetic drugs due to their unintended side effects, high costs, limited specificity, and toxicity, medicinal plants and their phytochemicals have gained significant attention as alternative potential chemotherapeutic agents [3, 10]. Phytochemicals possess antimicrobial, anticancer, and anti-inflammatory properties, making them promising alternative therapeutics [11]. Their low cost, increased accessibility, and limited side effects enhance their suitability compared to synthetic drugs [12]. The antiproliferative properties of phytochemicals are attributed to their ability to modulate signalling pathways, promote cell cycle arrest and apoptosis, inactivate carcinogens, inhibit proliferation, and regulate the immune system [11, 13]. Ginger (*Zingiber officinale*) is a medicinal plant that possesses pharmacological properties and elicits its therapeutic effects as a result of its phytochemicals, namely: 6-gingerol, 6-shogal and zingerone [14].

Zingerone (4-(4-hydroxy3-methoxyphenyl)-2-butanone), a bioactive phytochemical compound derived from ginger, exhibits pharmacological properties such as anti-inflammatory, antidiabetic, antidiarrhoeic, anticancer and antispasmodic properties [3]. Although limited studies have investigated the effect of zingerone on melanoma cells, its chemotherapeutic properties have been observed in malignancies such as prostate cancer, neuroblastoma, ovarian and colorectal cancer, where it was shown to exhibit antiproliferative properties by inducing cell cycle arrest and inhibiting angiogenesis [3, 15, 16].

Although phytochemicals show promising results as chemotherapeutic agents, their clinical use is limited due to their low bioavailability and the high dose required to achieve significant beneficial effects [3, 17, 18]. However, combining phytochemicals with conventional cytotoxic drugs has gained significant attention. This approach has the potential to reduce the synthetic drug dose, improve drug bioavailability, limit drug resistance and maximise the synergistic effects of phytochemicals with synthetic drugs to inhibit cancer growth and proliferation [3, 19].

To our knowledge, limited studies have investigated the effect of combining MAZ-51 and zingerone on melanoma proliferation. Additionally, these compounds target distinct mechanistic pathways. Therefore, it is beneficial to explore the impact of combination treatment with both compounds to inhibit tumour cell proliferation, as melanoma utilises multiple signalling pathways to promote proliferation and survival and is known to evade attempts to inhibit one signalling pathway by activating another [20]. Therefore, this study aimed to investigate the individual and combined effects of MAZ-51 and zingerone on melanoma cell proliferation using a cell survival assay, microscopy and flow cytometry to identify cell cycle changes.

2 | Methodology

2.1 | Ethics approval

Ethics approval for this study was granted by the University of Pretoria's Faculty of Health Science Research Ethics Committee (Ethics committee number: 192/2022).

2.2 | Cell Lines: Melanoma and Keratinocyte Cell Lines

B16-F10 melanoma, a highly metastatic cell line, expresses the receptors CXCR4 and VEGFR-3 and was purchased from the

American Type Culture Collection (ATCC CRL-6475). It is a murine cell line produced as the 10th serial passage subclone of the B16 parent tumour line in the C57BL/6J mice strain [21]. The HaCaT cell line is a non-tumourigenic monoclonal human keratinocyte cell line that is derived from an adult human skin. The cell line exhibits a partially to fully differentiated phenotype. The cell line was purchased from CELLONEX, South Africa and served as a control cell line [22]. The B16-F10 and HaCaT cells were utilised from passages 2–12 and passages 45–55, respectively.

2.3 | Sample Preparation

MAZ-51 and zingerone were dissolved in dimethyl sulfoxide (DMSO) with a final concentration of less than 0.1% (w/v). Serial dilutions were made by adding ddH_2O to the compounds. Control samples were treated with a vehicle control of 0.01% DMSO (v/v). An additional control sample at 0.6% DMSO (v/v) and a medium control sample were included following the calculation of the maximal inhibitory concentrations (IC_{50}) to account for the increased DMSO concentration for zingerone at IC_{50} values. However, nonsignificant differences were recorded between the controls; therefore, 0.01% DMSO was used as the standard control. The concentration ranges utilised in this study were selected from previous literature and were further optimised to yield optimal results for this study [15, 23]. Cells were treated with MAZ-51 (0.002–0.005 mg/mL), zingerone (0.5–2 mg/mL) and nocodazole (NOC) at 0.004 mg/mL for 24, 48 and 72 h. Nocodazole served as a positive control, as it is known to result in a G_2/M mitotic phase block [24]. Following the determination of the IC_{50} values, subsequent experimental assays were performed at 48 and 72 h due to nonsignificant data observed at 24 h. Cells were treated with IC_{50} values of MAZ-51, zingerone, and a combination of MAZ-51 and zingerone.

2.4 | Cell Culture

The cells were grown in T25 or T75cm^2 culture flasks and were maintained in Dulbecco's modified Eagle's medium (DMEM) (Whitehead Scientific, Brackenfell, Cape Town, South Africa), supplemented with 10% heat-inactivated foetal calf serum (FCS) and 1% penicillin/streptomycin to form complete culture medium (CCM). Cells were then stored in a humidified Forma Scientific water-jacketed incubator at 37°C and 5% CO_2. Cell growth was monitored daily, with CCM changes taking place every 2–3 days.

After reaching 70%–90% confluency, the B16-F10 and HaCaT cells were sub-cultured by removing the medium, gently washed twice with 3 mL of 1 × phosphate buffered saline (PBS) and a dissociation agent, namely TrypLE Express phenol red, and 5% trypsin was utilised to aid B16-F10 and HaCaT cell detachment respectively. This was followed by incubation for 3–5 min. Thereafter, 5 mL of CCM was added to the cell suspension to inactivate the TrypLE Express phenol red and 5% trypsin. The cell suspension was transferred to a 15 mL tube and centrifuged for 5 min at 1429 × *g*. Following centrifugation, the supernatant was discarded, followed by resuspension with 1 mL of CCM.

2.5 | Spectrophotometry

2.5.1 | Determination of Cell Viability: Crystal Violet

B16-F10 and HaCaT cells were seeded at a volume of 0.09 mL and concentrations of 5×10^4 cells/mL (5×10^3 cells/well) and 10×10^4 cells/mL (9×10^3 cells/well) respectively in 96-well plates and allowed to attach overnight. Cells were treated with the compounds: zingerone (0.5–2 mg/mL), MAZ-51 (0.002–0.005 mg/mL) and NOC, a positive control, at 0.004 mg/mL, followed by incubation for 24, 48 and 72 h. Following incubation, termination was aided by the addition of 200 μL of 1% glutaraldehyde dissolved in ddH_2O to the 96 well plates. The plates were incubated for 30 min followed by the removal of glutaraldehyde. Crystal violet, 100 μL of 0.1% solution, was dissolved in ddH_2O and added to stain the plates for 30 min at room temperature (RT) followed by rinsing of the plates under running water. The plate was left to dry overnight followed by the addition of 100 μL of 10% acetic acid dissolved in ddH_2O to solubilise the crystal violet dye. The absorbance was read at 630 nm using a spectrophotometer ELx800 Universal Microplate Reader (Bio-Tek Instruments Inc.) The results were reported as a percentage of cell viability against the vehicle control group.

2.6 | Combination Index Calculation

The following combination index (CI) formula was utilised to determine whether the combination treatment of MAZ-51 and zingerone resulted in a synergistic, antagonistic, or additive effect. A CI that is greater than, less than, or equal to one indicates an antagonistic, synergistic, or additive effect respectively [25].

$$CI = C_{A,x} / IC_A + C_{B,x} / IC_B$$

where $C_{A,x}$ is the concentration of compound A at which a cytotoxic effect is observed and IC_A is the IC_{50} of compound A. $C_{B,x}$ is the concentration of compound B at which a cytotoxic effect is observed and IC_B is the IC_{50} of compound B. If the CI is equal to 1, there is an additive effect; if the CI is above 1, there is an antagonistic effect; and if CI is below 1, there is a synergistic effect [25].

2.7 | Determination of Cell Morphology

2.7.1 | Polarisation Optical Differential Inferential Contrast and Haematoxylin and Eosin Staining

The cells were seeded on heat-sterilised coverslips in a 24-well plate at a volume of 0.45 mL and concentrations of 10×10^4 cells/mL (4.5×10^4 cells/well) and 20×10^4 cells/mL (9×10^4 cells/well) for the B16-F10 and HaCaT cells respectively and were left to attach overnight. Following overnight incubation,

cells were exposed to the different compounds: NOC, MAZ-51, zingerone and a combination of MAZ-51 and zingerone at the calculated B16-F10 IC_{50} values for 48 and 72 h. For PlasDIC, images were taken using the Zeiss inverted microscope (Axiovert CFL40 Zeiss; Oberkochen, Germany). Following PlasDIC, the CCM was removed, and the cells were fixed with Bouin's fixative for an hour. Bouin's fixative was removed, and 70% ethanol was added to the coverslips for 20 min at RT. Coverslips were then rinsed for 2 min with tap water followed by the addition of Mayer's haematoxylin for 20 min and rinsing under tap water for 2 min. Coverslips were treated with 70% ethanol followed by the addition of 1% eosin dissolved in ddH_2O for 5 min. The eosin was removed, and the coverslips were dehydrated twice with increasing concentrations of ethanol at 70%, 96% and 100% followed by the addition of xylene. Coverslips were mounted on microscope slides with resin and were left to dry. Zeiss Axiovert MRc microscope (Zeiss, Oberkochen, Germany) was used to acquire images at 100× magnification with immersion oil.

2.8 | Flow Cytometry

2.8.1 | Cell Cycle Analysis

B16-F10 and HaCaT cells were seeded in a 24-well plate at a volume of 0.45 mL and concentrations of 10×10^4 cells/mL (4.5×10^4 cells/well) and 20×10^4 cells/mL (9×10^4 cells/well) respectively, and allowed to attach overnight. Cells were treated with NOC, zingerone, MAZ-51, and a combination of zingerone and MAZ-51 at the B16-F10 IC_{50} values for 48 and 72 h, followed by trypsinisation and resuspension in 1 mL of CCM. The cells were centrifuged for 5 min at 1429× g, followed by resuspension of the pellet with 200 µL ice-cold PBS. The cells were centrifuged for 5 min, and the supernatant was discarded. Cells were treated with 70% methanol that was added in a drop-wise manner and stored at −20°C before analysis took place. Prior to analysis, cells were pelleted by centrifuging them for 5 min at 1429× *g*. The supernatant was removed, followed by washing the cells in a 0.5% bovine serum albumin (BSA)/PBS solution. Cells were resuspended in 1 mL of PBS that contains propidium iodide (PI) (40 µg/mL), 100 µg/mL RNase A and 0.1% triton-X, and incubated at 37°C, 5% CO_2 for 45 min. An FC500 flow cytometer (Beckman Coulter, Johannesburg, South Africa) was used for cell analysis. Distribution of the cell cycle was calculated using Kaluza C software (version 1.2.1) by allocating deoxyribonucleic acid (DNA) content per cell to sub-G_1, G_1, S and G_2/M phases.

2.9 | The Effect of a Growth Factor on Cell Numbers

2.9.1 | Vascular Endothelial Growth Factor

B16-F10 and HaCaT cells were seeded at a volume of 0.09 mL and concentrations of 5×10^4 cells/mL (5×10^3 cells/well) and 10×10^4 cells/mL (9×10^3 cells/well) respectively, in a 96-well plate. Cells were exposed to MAZ-51, zingerone, and a combination of MAZ-51 and zingerone at the B16-F10 IC_{50}. Cells were further exposed to either 20 or 60 ng/mL of vascular endothelial growth factor (VEGF) (Sigma-Aldrich, Kempton Park, South Africa) for the stipulated time period of 48–72 h. Additional control samples were included, either exposed to VEGF or not exposed to VEGF at 20 or 60 ng/mL. Crystal violet analysis was then carried out in the same manner as explained in Section 2.5.1.

2.10 | Statistical Analysis

Each experiment was performed with three technical and three biological repeats for all cell lines and was tested for normality using the Shapiro–Wilk test. Data obtained from quantitative experiments are represented by the mean ± standard error of the mean (SEM) and statistically analysed using the one-way analysis of variance (ANOVA). The Bonferroni test was used as a post hoc test for all pairwise analyses and $p \leq 0.05$ was considered statistically significant. GraphPad Prism version 9.5.1 was utilised for statistical analysis.

3 | Results

3.1 | Crystal Violet Staining of B16-F10 and HaCaT Cells: Zingerone and MAZ-51 Induced a Decrease in Cell Viability

The effects of the compounds MAZ-51 and zingerone at concentration ranges of 0.002–0.005 and 0.5–2 mg/mL, respectively were evaluated on the B16-F10 melanoma and HaCaT human keratinocyte cell lines for viability for 24, 48 and 72 h.

Zingerone-treated B16-F10 cells significantly decreased cell numbers from concentrations of 1.5–2 and 0.5–2 mg/mL for 48 and 72 h, respectively ($p < 0.05$; Figure 1A) whereas HaCaT cells displayed a significant decrease in cell numbers at concentrations of 1–2 mg/mL at 24, 48, and 72 h ($p < 0.05$; Figure 1C). A significant decrease in cell numbers was also observed in MAZ-51 treated B16-F10 cells from 0.004 and 0.005 mg/mL at 72 h ($p < 0.05$; Figure 1B). However, a nonsignificant decrease was observed in MAZ-51 treated HaCaT cells at 24, 48, and 72 h (Figure 1D).

The positive control, NOC, induced a significant decrease in cell numbers in the B16-F10 cells at 48 and 72 h ($p < 0.01$; Figure 1A) whereas a significant decrease at 24, 48, and 72 h was observed in the HaCaT cells ($p < 0.05$; Figure 1C,D).

The IC_{50} determined by linear regression for zingerone was 27.9, 2.199 and 1.219 mg/mL at 24, 48 and 72 h, respectively. The IC_{50} for MAZ-51 was 0.05428, 0.03162 and 0.01204 mg/mL at 24, 48 and 72 h, respectively (Table 1). Due to the non-statistical decrease in cell numbers observed at 24 h, subsequent experimental assays were conducted at 48 and 72 h. The IC_{50} values resulted in lower percentage cell numbers in the B16-F10 cell lines in comparison to the HaCaT cells at 48 h (Figure 2). However, at 72 h treatment with zingerone at IC_{50} and a combination of MAZ-51 and zingerone was more potent in the control cell lines

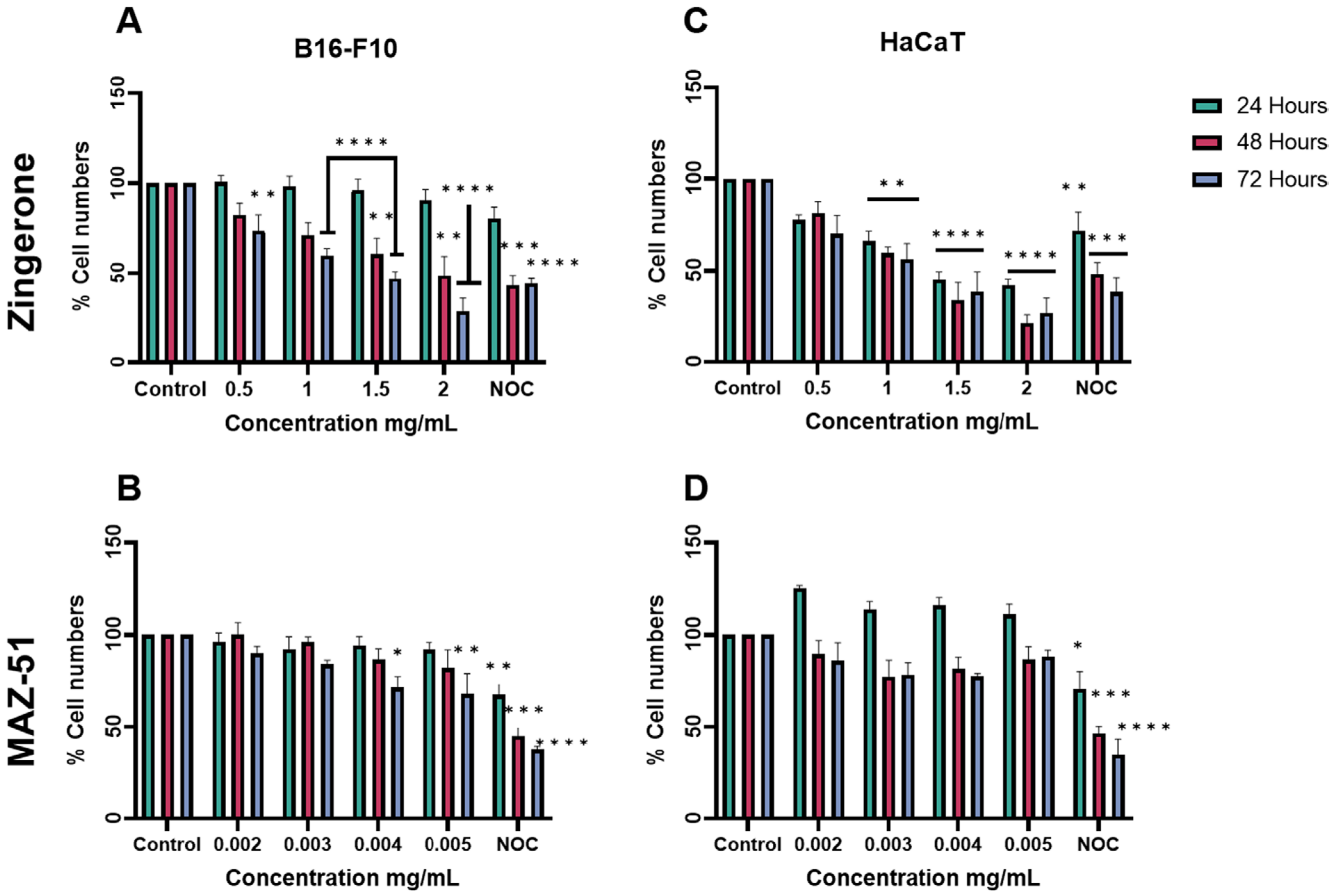

FIGURE 1 | The effect of zingerone and MAZ-51 on the cell number of the B16-F10 (A, B) and HaCaT (C, D) cells at 24, 48, and 72 h. *$p < 0.05$, **$p < 0.01$, ***$p < 0.001$, ****$p < 0.0001$ indicates significance in comparison to the control. Graphs were designed using GraphPad Prism version 9.5.1.

TABLE 1 | Table depicting the half maximal inhibitory concentrations (mg/mL) for the B16-F10 and HaCaT cell lines at 24, 48, and 72 h.

	B16-F10			HaCaTs		
	24 h	**48 h**	**72 h**	**24 h**	**48 h**	**72 h**
MAZ-51	0.05428	0.03162	0.01204	1.131E+51	1.557E+46	0.0176
Zingerone	27.9	2.199	1.219	1.548	1.074	1.027

compared to the B16-F10 cell lines (Figure 2). The combination treatments at IC_{50} resulted in a CI of 2 for both 48 and 72 h (Figure 3).

Due to the significant reduction in cell numbers observed in zingerone-treated HaCaT cells at IC_{50} values, the effects of zingerone at IC_{25} values (1.0995 mg/mL for 48 h and 0.60695 mg/mL for 72 h) were further investigated. This study also examined the combined treatment of MAZ-51 at IC_{50} and zingerone at IC_{25} concentrations in the B16-F10 and HaCaT cells. In comparison to the IC_{50} values, zingerone at IC_{25} values resulted in higher percentage cell numbers at both cell lines at 48 and 72 h ($p < 0.05$; Table 2). In addition, combination treatment also resulted in an increase in the percentage cell numbers ($p < 0.05$; Table 2) and CI of 1.5 for 48 and 72 h (Figure 3).

3.2 | Combination Index Calculation for MAZ-51 and Zingerone

This study calculated the CI for MAZ-51 and zingerone by utilising the concentrations at which the compounds inhibited 50% cell growth, which is tabulated on page 10 Table 1. Zingerone's IC_{25} values are tabulated in Table 2.

Combination Index Calculation for MAZ-51 at IC_{50} and zingerone at IC_{50}

CI at 48 h = 0.03162 mg/mL/0.03162 mg/mL + 2.199 mg/mL/2.199 mg/mL = 2.

CI at 72 h = 0.01204 mg/mL 0.01204 mg/mL + 1.219 mg/mL/1.219 mg/mL = 2.

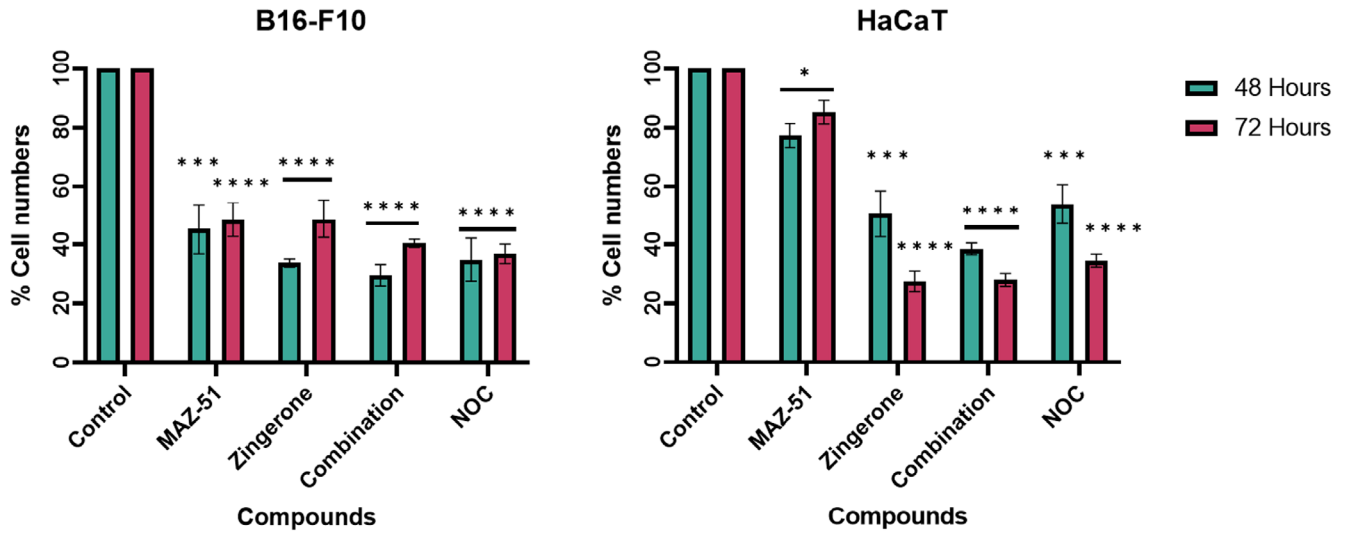

FIGURE 2 | The effect of the half maximal inhibitory concentrations of MAZ-51 and zingerone on the B16-F10 and HaCaT cells at 48 and 72 h. $^{*}p < 0.05$, $^{**}p < 0.01$, $^{***}p < 0.001$, $^{****}p < 0.0001$ indicates significance in comparison to the control. Graphs were designed using GraphPad Prism version 9.5.1.

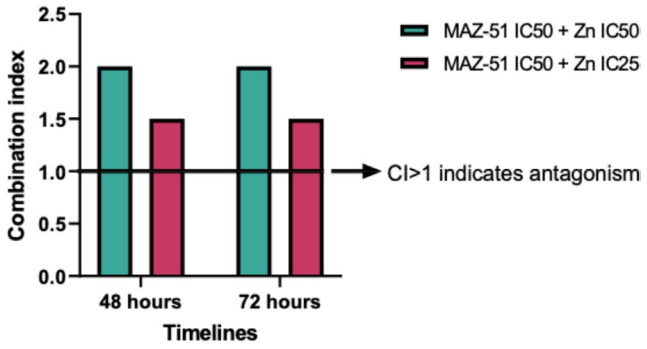

FIGURE 3 | Combination index (CI) recorded at 48 and 72 h for treatment with MAZ-51 (IC_{50}) + zingerone (IC_{50}) and MAZ-51 (IC_{50}) + zingerone (IC_{25}). A CI > 1 indicates antagonism between the two compounds. The CI was calculated using the B16-F10 melanoma cell's IC_{50}. Graph was designed using GraphPad Prism version 9.5.1.

Combination index calculation for MAZ-51 at IC_{50} and zingerone at IC_{25}

CI at 48 h = 0.03162 mg/mL/0.03162 mg/mL + 1.0995 mg/mL/2.199 mg/mL = 1.5.

CI at 72 h = 0.01204 mg/mL/0.01204 mg/mL + 0.6095 mg/mL/1.219 mg/mL = 1.5.

3.3 | The Effect of Zingerone and MAZ-51 on Cell Morphology

3.3.1 | Polarisation Optical Differential Inferential Contrast Imaging of B16-F10 and HaCaT Cells Treated With Zingerone and MAZ-51

In PlasDIC micrographs, B16-F10 melanoma cells treated with zingerone at IC_{50} values at 48 and 72 h exhibited apoptotic bodies and protrusions (Figures 4 and 5). Samples treated with MAZ-51 exhibited a decrease in density and cell rounding (Figures 4 and 5). Combination treatment at IC_{50} with MAZ-51 and zingerone resulted in apoptotic bodies and protrusions (Figures 4 and 5). NOC-treated samples revealed cell debris, cell swelling, and a decrease in density (Figures 4 and 5).

HaCaT cells treated with zingerone at IC_{50} at 48 and 72 h showed protrusions, whereas exposure to MAZ-51 led to the development of cell rounding and cell swelling (Figures 4 and 5). Combination treatment at IC_{50} resulted in protrusions. NOC-treated cells revealed cell swelling and debris (Figures 4 and 5).

3.3.2 | Haematoxylin and Eosin Staining of B16-F10 and HaCaT Cells Treated With Zingerone and MAZ-51

H&E-stained control B16-F10 melanoma cells exhibited confluent cells (Figures 6 and 7). Treatment with zingerone revealed protrusions and apoptotic bodies (Figures 6 and 7). MAZ-51-treated cells exhibited pyknosis, cell swelling, and a decrease in density (Figures 6 and 7). Combination treatment showed a decrease in density, protrusions, and cell swelling (Figures 6 and 7). NOC-treated samples resulted in cell swelling, membrane blebbing, and karyorrhexis (Figures 6 and 7).

H&E-stained HaCaT control cells at 48 and 72 h exhibit confluent cells (Figures 6 and 7). Cells treated with zingerone and a combination of zingerone and MAZ-51 exhibited protrusions. MAZ-51 treated cells resulted in karyorrhexis (Figures 6 and 7). NOC-treated cells revealed a decrease in density, cell swelling, membrane blebbing, and karyorrhexis (Figures 6 and 7).

3.4 | Cell Cycle Analysis of B16-F10 and HaCaT Cells

3.4.1 | MAZ-51 and Zingerone Resulted in a Cell Cycle Arrest

Cell cycle analysis showed that there was a significant increase in the number of cells in the sub-G_1 phase in the B16-F10 cells treated with MAZ-51, zingerone, a combination of

TABLE 2 | Table comparing the effects of zingerone at IC_{50}, IC_{25}, and combination treatment on percentage cell numbers on the B16-F10 and HaCaT cell lines at 48 and 72 h.

		Treatment compounds			
		Zingerone		MAZ-51 + zingerone	
Timelines	Cell lines	Zn-IC_{50}	Zn-IC_{25}	MAZ-51 IC_{50} + Zn IC_{50}	MAZ-51 IC_{50} + Zn IC_{25}
48 h	B16-F10	34%**** (27.91–39.80)	47%**** (25.10–65.03)	30%**** (14.20–45.12)	46%**** (19.75–67.89)
	HaCaTs	50%*** (17.03–84.24)	51%** (18.06–104.4)	39%**** (29.93–47.34)	52%** (34.46–90.98)
72 h	B16-F10	49%**** (21.56–76.41)	53%**** (22.70–74.61)	41%**** (34.57–46.60)	60%*** (25.86–84.66)
	HaCaTs	28%**** (12.66–42.63)	61%** (52.46–93.36)	28%**** (18.53–37.64)	61%** (51.99–92.57)

Note: The confidence intervals are indicated in the brackets. *$p < 0.05$, **$p < 0.01$, ***$p < 0.001$, ****$p < 0.0001$ indicates significance in comparison to the control.

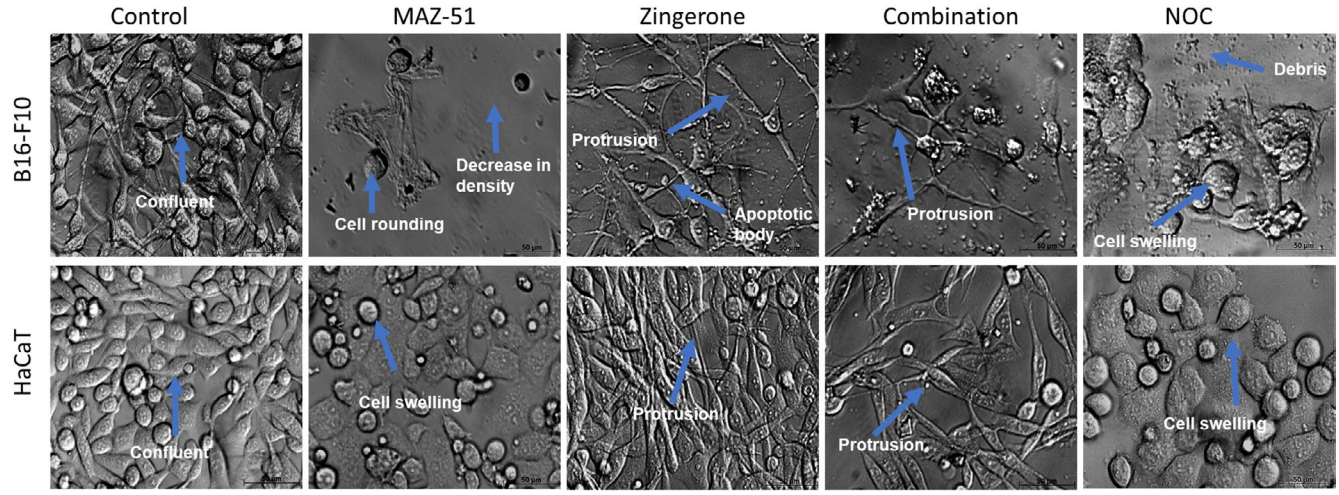

FIGURE 4 | Polarisation optical differential inferential contrast imaging of B16-F10 and HaCaT cells at 48 h. Images were taken at 40× magnification. Scale bar 50 μm.

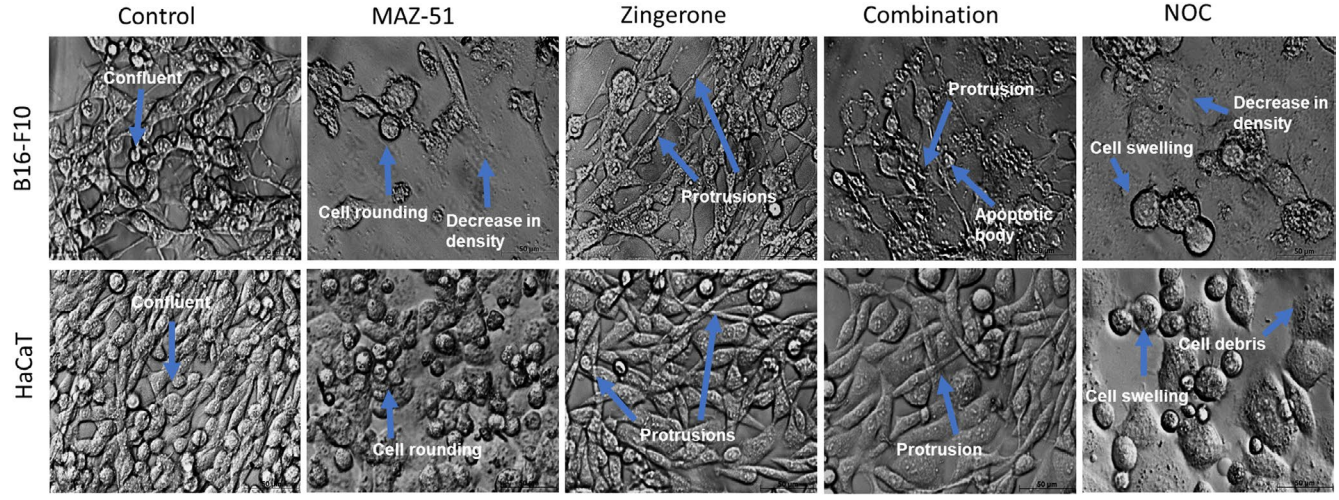

FIGURE 5 | Polarisation optical differential inferential contrast imaging of B16-F10 and HaCaT cells at 72 h. Images were taken at 40× magnification. Scale bar 50 μm.

zingerone and MAZ-51 at IC_{50} and NOC at 48 h. This was followed by a decrease in the number of cells in the G_1 phase ($p < 0.05$; Figure 8). At 48 h, HaCaT cells exhibited a significant increase ($p < 0.001$) in the number of zingerone and combination treated cells in the sub-G_1 phase, followed by a decrease in the number of cells in the G_1 phase ($p < 0.0001$; Figure 8). NOC-treated cells exhibited a significant increase ($p < 0.001$) in the number of cells in the G_2/M phase in the B16-F10 cells at 48 h and HaCaT cells at 48 and 72 h, indicative of a G_2/M cell cycle block.

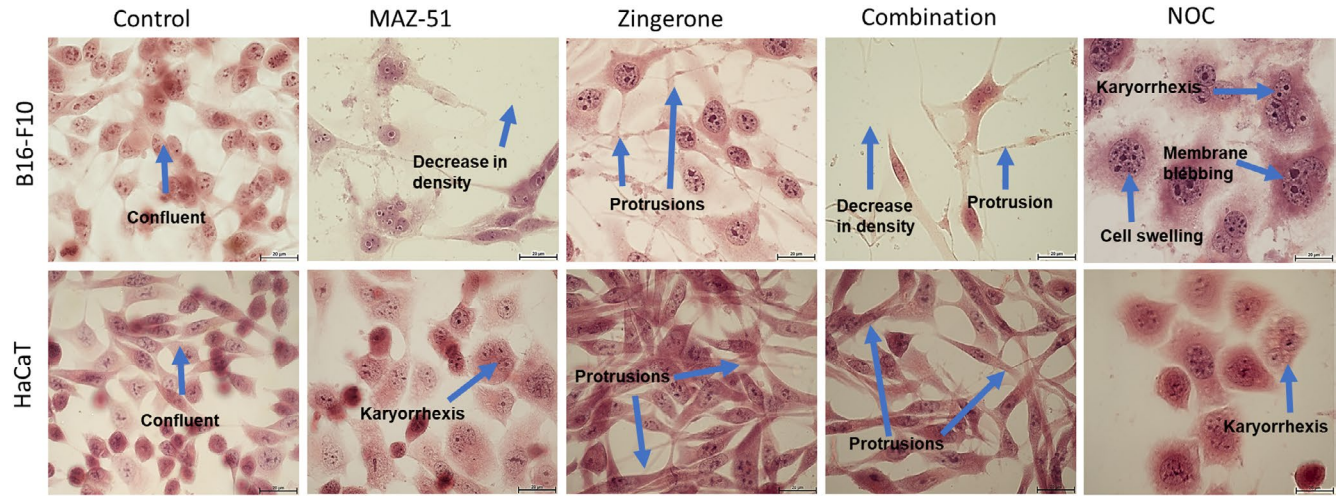

FIGURE 6 | Haematoxylin and eosin staining of B16-F10 and HaCaT cells at 48 h. Images were taken at 100× magnification. Scale bar 20 μm.

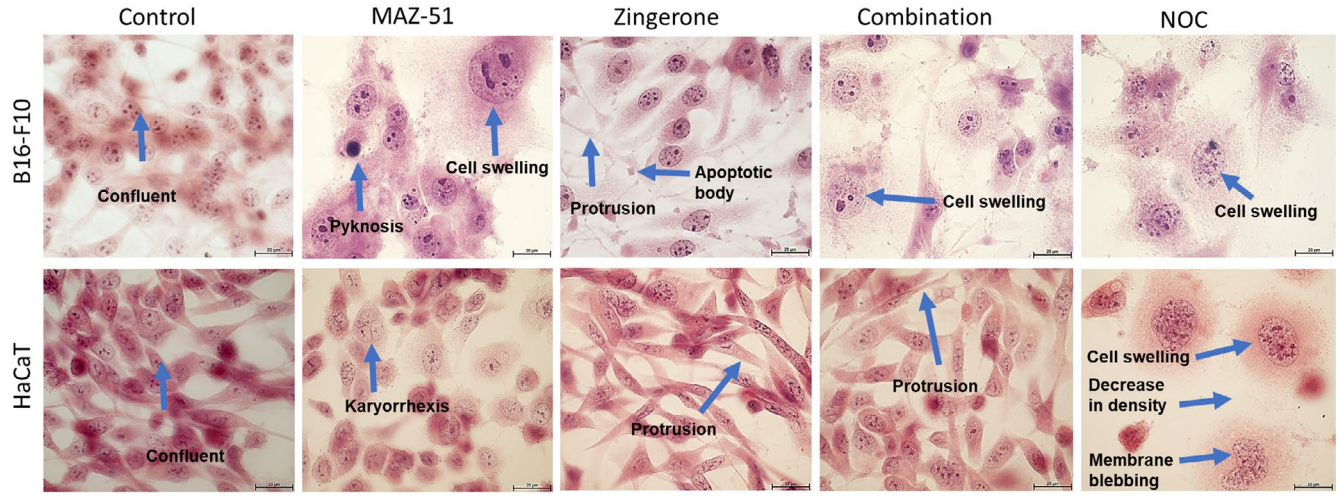

FIGURE 7 | Haematoxylin and eosin staining of B16-F10 and HaCaT cells at 72 h. Images were taken at 100× magnification. Scale bar 20 μm.

MAZ-51, zingerone, and combination treatment at IC_{50} had no significant effect on the B16-F10 cells at 72 h. HaCaT cells treated with zingerone and combination treatment at IC_{50} resulted in a significant increase ($p < 0.01$) in cell numbers in the sub-G_1 phase at 72 h. This was followed by a significant decrease ($p < 0.001$) in cell numbers in the G_1 phase (Figure 8). MAZ-51-treated HaCaT cells resulted in a significant decrease ($p < 0.01$) in cell numbers in the G_1 phase at 72 h (Figure 8).

3.5 | The Effects of Vascular Endothelial Growth Factor on the B16-F10 and HaCaT Cells

B16-F10 cells treated with MAZ-51 and VEGF at 20 and 60 ng/mL (MAZ-51/VEGF+) resulted in an increase in the percentage number of cells at 48 and 72 h in comparison to cells that were only treated with MAZ-51 (MAZ-51/VEGF−) ($p < 0.05$; Tables 3 and 4). However, MAZ-51/VEGF+ resulted in a decrease in cell numbers in the HaCaT cells at 48 and 72 h (Tables 3 and 4). Zingerone/VEGF+ and combination treatment/VEGF+ treated B16-F10 cells resulted in a decrease in percentage cell numbers compared to the VEGF− cells at 48 and 72 h ($p < 0.0001$; Tables 3 and 4). HaCaT cells exhibited a decrease in percentage cell numbers in zingerone/VEGF+ and combination/VEGF+ cells at 48 h ($p < 0.0001$; Tables 3 and 4) however, an increase in cell numbers was observed at 72 h in comparison to the VEGF− cells ($p < 0.001$; Tables 3 and 4).

4 | Discussion

The global incidence of cancer continues to rise; as such, there is a need to develop novel treatment strategies. Phytochemicals have acquired substantial attention as adjuvant therapy to inhibit cancer growth without eliciting cytotoxic effects on noncancerous cells [3]. Therefore, this study investigated the individual and combined effects of MAZ-51 and zingerone on melanoma cell proliferation. The study findings indicate that MAZ-51 and zingerone are cytotoxic to the B16-F10 melanoma cells. In addition, the compounds induced morphological changes indicating cell death and resulted in a cell-cycle arrest.

Consistent with results obtained by Scholtz and Mabeta who recorded a significant decrease in the cell viability of

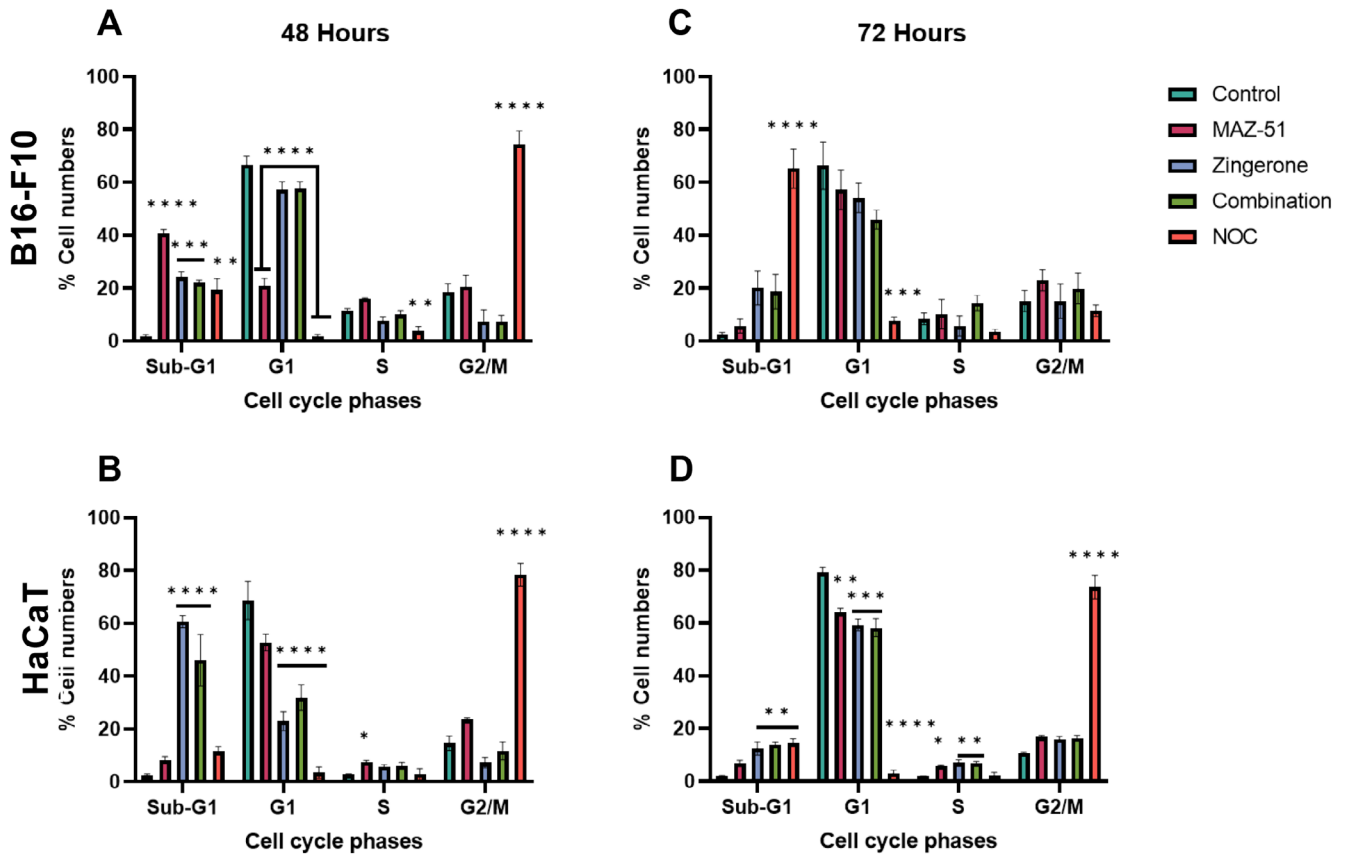

FIGURE 8 | The effect of the half maximal inhibitory concentrations of MAZ-51 and zingerone on the B16-F10 and HaCaT cells on cell cycle progression at 48 and 72 h. *$p < 0.05$, **$p < 0.01$, ***$p < 0.001$, ****$p < 0.0001$ indicates significance in comparison to the control. Graphs were designed using GraphPad Prism version 9.5.1.

endothelial and B16-F10 melanoma cells treated with MAZ-51 [23], this study observed a significant decrease in cell numbers in B16-F10 cells at 72 h at concentrations of 0.004 and 0.005 mg/mL. MAZ-51 had no significant effect on the HaCaT cells at 24, 48 and 72 h, thus demonstrating differential toxicity in the cell lines. This is further confirmed by the experimental IC_{50} data, where MAZ-51 reduced cell numbers to 45% ($p < 0.001$) and 49% ($p < 0.0001$) at 48 and 72 h, respectively in the B16-F10 cells. In the HaCaT cells, MAZ-51 reduced cell numbers to 77% ($p < 0.05$) and 85% ($p < 0.05$) at 48 and 72 h, respectively. This data indicates that MAZ-51 is cytotoxic; however, it is more potent in the B16-F10 cells compared to the HaCaT cells, suggesting its specificity to transformed cancerous cells.

Current literature supports the use of phytochemicals as potential cancer treatments, suggesting that they will result in therapeutic effects, with limited cytotoxicity to noncancerous cells compared to current synthetic drugs [26, 27]. However, this study observed that zingerone was more cytotoxic to the B16-F10 and HaCaT cells compared to treatment with MAZ-51. The literature also states that phytochemicals are required at higher concentrations to elicit therapeutic effects in cancer cells [17, 18]. Findings from this study indicate that the increased concentrations of zingerone decreased the B16-F10 cell numbers. An enhanced cytotoxic effect was observed in the noncancerous HaCaT cell lines at IC_{50} at 48 and 72 h, with enhanced toxicity observed at 72 h. To combat this, zingerone's IC_{25} was determined and increased the HaCaT cell numbers, indicating a potential therapeutic concentration. In addition, zingerone at 48 h was more cytotoxic to the B16-F10 compared to at 72 h. This demonstrates that treatment at 48 h yielded optimal cytotoxic effects in the B16-F10 cells with reduced toxicity exerted on the HaCaT cells. To elucidate the additional characteristics of the compounds of interest, morphological studies were done on the B16-F10 and HaCaT cells treated with MAZ-51, zingerone, and a combination of MAZ-51 and zingerone at IC_{50} at 48 and 72 h.

Morphological observations using PlasDIC and H&E staining showed the formation of cellular protrusions and apoptotic bodies in zingerone-treated cells. This observation is in agreement with findings by Chu et al., who observed cytoskeleton elongations and dendrite-like structures in zingerone-treated B16-F10 cells [28]. Consistent with results recorded by Park et al. in glioma cells [29], MAZ-51-treated B16-F10 and HaCaT cells exhibited cell rounding, karyorrhexis, pyknosis, and cell swelling, which are characteristic of apoptosis and necrosis. The morphology data indicate that MAZ-51 and zingerone are cytotoxic and induce structural changes that indicate cell death. Since the study observed structural changes that are characteristic of both apoptosis and necrosis, the type of cell death induced by the compounds needs to be further investigated. To further examine the effects of MAZ-51 and zingerone on melanoma growth and proliferation, flow cytometry analysis was used to determine the effects of the compounds on cell cycle progression.

TABLE 3 | Table depicting the effect of vascular endothelial growth factor at 20 ng/mL on percentage cell numbers in the B16-F10 and HaCaT cells at 48 and 72 h.

		Treatment compounds					
		MAZ-51		Zingerone		MAZ-51 + Zingerone	
Timelines	Cell lines	VEGF−	VEGF+	VEGF−	VEGF+	VEGF−	VEGF+
48 h	B16-F10	45%*** (9.176–81.60)	69%* (21.62–116.1)	34%**** (27.91–39.80)	19%**** (17.30–19.71)	30%**** (14.20–45.12)	18%**** (4.456–31.19)
	HaCats	77%* (58.99–94.70)	70%** (42.59–98.17)	51%*** (17.03–84.24)	30%**** (9.906–50.48)	39%**** (29.93–47.34)	31%**** (7.266–54.15)
72 h	B16-F10	48%**** (23.47–73.99)	64%** (33.56–93.45)	49%**** (21.56–76.41)	35%**** (26.51–44.03)	41%**** (34.57–46.60)	35%**** (21.60–49.30)
	HaCaTs	85%* (67.93–102.4)	76% (43.81–107.5)	28%**** (12.66–42.63)	43%*** (9.769–75.93)	28%**** (18.53–37.64)	35%**** (15.27–54.66)

Note: The confidence intervals are indicated in the brackets. *$p < 0.05$, **$p < 0.01$, ***$p < 0.001$, ****$p < 0.0001$ indicate significance in comparison to the control.

TABLE 4 | Table depicting the effect of vascular endothelial growth factor at 60 ng/mL on percentage cell numbers in the B16-F10 and HaCaT cells at 48 and 72 h.

		Treatment compounds					
		MAZ-51		Zingerone		MAZ-51 + Zingerone	
Timelines	Cell lines	VEGF−	VEGF+	VEGF−	VEGF+	VEGF−	VEGF+
48 h	B16-F10	45%*** (9.176–81.60)	66%*** (46.25–85.07)	34%**** (27.91–39.80)	19%**** (15.40–22.98)	30%**** (14.20–45.12)	18%**** (2.740–33.62)
	HaCaTs	77%* (58.99–94.70)	68%* (41.68–93.70)	51%*** (17.03–84.24)	38%**** (11.44–64.29)	39%**** (29.93–47.34)	43%**** (17.44–69.06)
72 h	B16-F10	48%**** (23.47–73.99)	65%** (37.94–91.29)	49%**** (21.56–76.41)	39%**** (31.70–45.80)	41%**** (34.57–46.60)	39%**** (25.79–52.83)
	HaCaTs	85%* (67.93–102.4)	80% (61.05–97.96)	28%**** (12.66–42.63)	45%**** (15.11–74.35)	28%**** (18.53–37.64)	37%**** (14.07–59.84)

Note: The confidence intervals are indicated in the brackets. *$p < 0.05$, **$p < 0.01$, ***$p < 0.001$, ****$p < 0.0001$ indicates significance in comparison to the control.

Flow cytometry analysis exhibited a significant increase in the number of cells in the sub-G_1 phase of B16-F10 cells treated with MAZ-51 at 48 h, and a non-significant effect was observed at 72 h. MAZ-51 at 72 h displayed non-significant effects on cell cycle progression in the B16-F10 cells. HaCaT cells treated with MAZ-51 at 48 and 72 h exhibited a non-significant increase in cells in the sub-G_1 phase, followed by a significant decrease in cell numbers in the G_1 phase at 72 h. This indicates that MAZ-51 inhibits HaCaT cell proliferation without inducing cell death. These findings are supported by results obtained by Park et al., who observed the effects of MAZ-51 on the rat C6 and human U251MG glioma cells, where the cytotoxic effects of MAZ-51 were non-significant on the control cell lines [29]. This indicates that MAZ-51 possesses antiproliferative properties; however, its cytotoxic properties target transformed cells. In addition, as MAZ-51 induced significant changes at 48 h in the B16-F10, with limited toxicity observed in the HaCaTs at 48 h, this indicates that treatment at this timeline yields maximal results, which is confirmed by the cell viability data.

Zingerone-treated B16-F10 cells resulted in a significant increase in the percentage of cells in the sub-G_1 phase at 48 h, with a less potent increase observed at 72 h. Similar results were observed in zingerone-treated HaCaT cells. Choi et al. observed an increase in the number of cells in prometaphase and a decrease in cells in metaphase in zingerone-treated neuroblastoma cells, indicating a mitotic arrest [15]. This data indicates that zingerone is cytotoxic to the B16-F10 and HaCaT cells. The quantitative flow cytometry data is supported by the qualitative data, suggesting that zingerone is toxic to the cells and induces apoptosis.

Angiogenic and lymphangiogenic factors such as VEGFs and their corresponding receptors are dysregulated during carcinogenesis and thus are critical targets for cancer therapy [29]. MAZ-51 inhibits VEGF-C-induced phosphorylation of VEGFR-3, inhibiting proliferation [30]. This study observed an increase in cell numbers in MAZ-51/VEGF+ cells compared to MAZ-51/VEGF− in the B16-F10 cells. Even though this study utilised non-specific VEGF, the findings provide a potential mechanism of action utilised by the treating compounds to inhibit cell proliferation and survival. Given that MAZ-51 specifically targets VEGFR-3, the results suggest that the additional VEGF activates alternative signalling pathways such as VEGFR-2 [30] that are activated in melanoma progression, thus explaining the increase in cell numbers observed in MAZ-51/VEGF+ cells compared to MAZ-51/VEGF− cells. Conversely, zingerone-treated B16-F10 cells supplemented with VEGF resulted in a decrease in cell numbers compared to VEGF− cells. This is supported by the results by Kung et al., who recorded a decrease in VEGF and VEGFR expression in endothelial cells treated with zingerone nanoparticles [31]. This data suggests that zingerone is cytotoxic in the presence of VEGF, indicating that it diminishes proliferation and survival by targeting VEGFs.

Literature recommends the use of phytochemicals as an alternative treatment for cancer due to their potential therapeutic value. Literature has highlighted that the individual use of phytochemicals often exhibits limited bioavailability and requires high concentrations to induce cytotoxic effects. When combined with pharmacological agents, phytochemicals demonstrate enhanced anti-inflammatory and antioxidant properties [3]. This study investigated the combined effects of MAZ-51 and zingerone on melanoma cell proliferation. The findings revealed that combination treatment significantly decreased cell numbers, induced morphological changes such as cellular protrusions and cell rounding, and caused a mitotic block in the B16-F10 melanoma cells.

However, this study recorded a combination index (CI) that is greater than one, indicating antagonism, at both inhibitory concentrations (IC_{50} and IC_{25}) and timelines. The consistently elevated CI indicates that the antagonistic effects of MAZ-51 and zingerone are independent of the compound concentrations but are possibly reliant on the mechanistic interactions of the compounds and thus, further indicates the incompatibility of MAZ-51 and zingerone. This antagonistic effect may be attributed to phytochemical-drug interactions that alter drug metabolising enzymes or transport proteins, modification of the chemotherapeutic by the phytochemical and incompatibility of the two drugs, resulting in the modification of the physical properties of the drugs such as drug solubility and stability [3, 32]. Previous studies have reported additive or synergistic effects of phytochemicals with pharmacological agents, supporting their role as adjuvant therapies. However, the antagonistic effects observed in this study highlight the significance of performing phytochemical-drug compatibility studies by carefully evaluating drug interactions, delivery mechanisms and compound compatibility [13, 33]. Given the above results, we recommend that future studies investigating the anticancer effects of MAZ-51 and zingerone should consider an individual compound approach to optimise therapeutic outcomes. In addition, as both zingerone and MAZ-51 individually possess chemotherapeutic properties, other combination therapies with phytochemicals and the use of nanoparticles may be explored to further enhance their chemotherapeutic effects. Zingerone has effectively inhibited the growth and proliferation of cancers such as neuroblastoma, prostate cancer and breast cancer, thus indicating its potential as a cancer therapeutic [15, 16, 34].

5 | Conclusion

In conclusion, the findings of this study demonstrate that MAZ-51 and zingerone effectively inhibit melanoma cell proliferation and survival, with zingerone showing promise as a potential therapeutic agent for melanoma treatment. While cytotoxic effects were observed at zingerone IC_{50} in both B16-F10 and HaCaT cells, treatment at IC_{25} significantly inhibited B16-F10 cell proliferation while exhibiting reduced toxicity in HaCaT cells. The results underscore the potential of zingerone as an alternative treatment option. However, due to the observed antagonistic interaction between MAZ-51 and zingerone both at IC_{50} and IC_{25} (resulting in a CI that is greater than one), we recommend that future studies investigate the individual effects of MAZ-51 at IC_{50} and zingerone at IC_{25}. Given that melanoma relies on the interplay of various signalling pathways to promote proliferation and survival, we recommend that future studies investigate the effects of zingerone on prominent signalling pathways such as CXCR4/CXCL12, VEGFR-3/VEGF-C, and TGF-β/TGFβRI to further elucidate the mechanistic action undertaken by the compounds to inhibit melanoma progression.

Author Contributions

Kganya Letsoalo: experimental and data analysis (lead); conceptualisation (equal), writing – original draft (lead), writing – review and editing (equal). **Charlise Basson:** writing – review and editing (equal). **Trevor Nyakudya:** conceptualisation (equal), writing – review and editing (equal). **Yvette Hlophe:** conceptualisation (equal), writing – review and editing (equal).

Conflicts of Interest

The authors declare no conflicts of interest.

Data Availability Statement

The data that support the findings of this study are available from the corresponding author upon reasonable request.

Peer Review

The peer review history for this article is available at https://www.webofscience.com/api/gateway/wos/peer-review/10.1111/1440-1681.70059.

References

1. M. Fantini, M. Benvenuto, L. Masuelli, et al., "In Vitro and In Vivo Antitumoral Effects of Combinations of Polyphenols, or Polyphenols and Anticancer Drugs: Perspectives on Cancer Treatment," *International Journal of Molecular Sciences* 16, no. 5 (2015): 9236–9282, https://doi.org/10.3390/ijms16059236.

2. I. J. Sagbo and W. Otang-Mbeng, "Plants Used for the Traditional Management of Cancer in the Eastern Cape Province of South Africa: A Review of Ethnobotanical Surveys, Ethnopharmacological Studies and Active Phytochemicals," *Molecules* 26, no. 15 (2021): 4639, https://doi.org/10.3390/molecules26154639.

3. K. Letsoalo, E. Nortje, S. Patrick, T. Nyakudya, and Y. Hlophe, "Decoding the Synergistic Potential of MAZ-51 and Zingerone as Therapy for Melanoma Treatment in Alignment With Sustainable Development Goals," *Cell Biochemistry and Function* 42, no. 2 (2024): e3950, https://doi.org/10.1002/cbf.3950.

4. R. Sever and J. S. Brugge, "Signal Transduction in Cancer," *Cold Spring Harbor Perspectives in Medicine* 5, no. 4 (2015): a006098, https://doi.org/10.1101/cshperspect.a006098.

5. W. Ju, H. H. Cai, W. Zheng, et al., "Cross-Talk Between Lymphangiogenesis and Malignant Melanoma Cells: New Opinions on Tumour Drainage and Immunization (Review)," *Oncology Letters* 27, no. 2 (2024): 81, https://doi.org/10.3892/ol.2024.14215.

6. V. Kirkin, R. Mazitschek, J. Krishnan, et al., "Characterization of Indolinones Which Preferentially Inhibit VEGF-C- and VEGF-D-Induced Activation of VEGFR-3 Rather Than VEGFR-2," *European Journal of Biochemistry* 268, no. 21 (2001): 5530–5540, https://doi.org/10.1046/j.1432-1033.2001.02476.x.

7. V. Kirkin, W. Thiele, P. Baumann, et al., "MAZ51, an Indolinone That Inhibits Endothelial Cell and Tumor Cell Growth in Vitro, Suppresses Tumor Growth in Vivo," *International Journal of Cancer* 112, no. 6 (2004): 986–993, https://doi.org/10.1002/ijc.20509.

8. P. Garcia-Oliveira, P. Otero, A. G. Pereira, et al., "Status and Challenges of Plant-Anticancer Compounds in Cancer Treatment," *Pharmaceuticals (Basel)* 14, no. 2 (2021): 157, https://doi.org/10.3390/ph14020157.

9. K. Sak, "Chemotherapy and Dietary Phytochemical Agents," *Chemotherapy Research and Practice* 2012 (2012): 282570, https://doi.org/10.1155/2012/282570.

10. A. I. Alqosaibi, "Nanocarriers for Anticancer Drugs: Challenges and Perspectives," *Saudi Journal of Biological Sciences* 29, no. 6 (2022): 103298, https://doi.org/10.1016/j.sjbs.2022.103298.

11. A. S. Choudhari, P. C. Mandave, M. Deshpande, P. Ranjekar, and O. Prakash, "Phytochemicals in Cancer Treatment: From Preclinical Studies to Clinical Practice," *Frontiers in Pharmacology* 10 (2019): 1614, https://doi.org/10.3389/fphar.2019.01614.

12. A. Sofowora, E. Ogunbodede, and A. Onayade, "The Role and Place of Medicinal Plants in the Strategies for Disease Prevention," *African Journal of Traditional, Complementary, and Alternative Medicines* 10, no. 5 (2013): 210–229, https://doi.org/10.4314/ajtcam.v10i5.2.

13. M. Ayaz, A. Nawaz, S. Ahmad, et al., "Underlying Anticancer Mechanisms and Synergistic Combinations of Phytochemicals With Cancer Chemotherapeutics: Potential Benefits and Risks," *Journal of Food Quality* 2022, no. 1 (2022): 1189034.

14. M. Nikkhah Bodagh, I. Maleki, and A. Hekmatdoost, "Ginger in Gastrointestinal Disorders: A Systematic Review of Clinical Trials," *Food Science & Nutrition* 7, no. 1 (2019): 96–108, https://doi.org/10.1002/fsn3.807.

15. J. S. Choi, J. Ryu, W. Y. Bae, et al., "Zingerone Suppresses Tumor Development Through Decreasing Cyclin D1 Expression and Inducing Mitotic Arrest," *International Journal of Molecular Sciences* 19, no. 9 (2018): 2832, https://doi.org/10.3390/ijms19092832.

16. S. Qian, H. Fang, L. Zheng, and M. Liu, "Zingerone Suppresses Cell Proliferation via Inducing Cellular Apoptosis and Inhibition of the PI3K/AKT/mTOR Signaling Pathway in Human Prostate Cancer PC-3 Cells," *Journal of Biochemical and Molecular Toxicology* 35, no. 1 (2021): e22611, https://doi.org/10.1002/jbt.22611.

17. M. Russo, C. Spagnuolo, I. Tedesco, and G. L. Russo, "Phytochemicals in Cancer Prevention and Therapy: Truth or Dare?," *Toxins (Basel)* 2, no. 4 (2010): 517–551, https://doi.org/10.3390/toxins2040517.

18. B. Rizeq, I. Gupta, J. Ilesanmi, M. AlSafran, M. M. Rahman, and A. Ouhtit, "The Power of Phytochemicals Combination in Cancer Chemoprevention," *Journal of Cancer* 11, no. 15 (2020): 4521–4533, https://doi.org/10.7150/jca.34374.

19. S. Rodriguez, K. Skeet, T. Mehmetoglu-Gurbuz, et al., "Phytochemicals as an Alternative or Integrative Option, in Conjunction With Conventional Treatments for Hepatocellular Carcinoma," *Cancers (Basel)* 13, no. 22 (2021): 5753, https://doi.org/10.3390/cancers13225753.

20. K. S. Smalley, "Understanding Melanoma Signaling Networks as the Basis for Molecular Targeted Therapy," *Journal of Investigative Dermatology* 130, no. 1 (2010): 28–37, https://doi.org/10.1038/jid.2009.177.

21. S. Urs, "B16-F10: A Murine Melanoma Model," 2019, https://drugdevelopment.labcorp.com/industry-solutions/oncology/preclinical/tumor-spotlights/b16-f10-a-murine-melanoma-model.html.

22. V. G. Wilson, "Growth and Differentiation of HaCaT Keratinocytes," *Methods in Molecular Biology* 1195 (2014): 33–41, https://doi.org/10.1007/7651_2013_42.

23. W. Scholtz and P. Mabeta, "Sunitinib Malate Inhibits Hemangioma Cell Growth and Migration by Suppressing Focal Adhesion Kinase Signaling," *Journal of Applied Biomedicine* 18, no. 4 (2020): 143–151, https://doi.org/10.32725/jab.2020.019.

24. A. Kallas, M. Pook, M. Maimets, K. Zimmermann, and T. Maimets, "Nocodazole Treatment Decreases Expression of Pluripotency Markers Nanog and Oct4 in Human Embryonic Stem Cells," *PLoS One* 6, no. 4 (2011): e19114, https://doi.org/10.1371/journal.pone.0019114.

25. L. Zhao, J. L. Au, and M. G. Wientjes, "Comparison of Methods for Evaluating Drug-Drug Interaction," *Frontiers in Bioscience (Elite Edition)* 2, no. 1 (2010): 241–249, https://doi.org/10.2741/e86.

26. P. Kumar, N. Yadav, B. Chaudhary, et al., "Promises of Phytochemical Based Nano Drug Delivery Systems in the Management of Cancer,"

Chemico-Biological Interactions 351 (2022): 109745, https://doi.org/10.1016/j.cbi.2021.109745.

27. J. Iqbal, B. A. Abbasi, R. Ahmad, et al., "Potential Phytochemicals in the Fight Against Skin Cancer: Current Landscape and Future Perspectives," *Biomedicine & Pharmacotherapy* 109 (2019): 1381–1393, https://doi.org/10.1016/j.biopha.2018.10.107.

28. L. W. Chu, J. Y. Chen, Y. W. Chen, S. Hsieh, and M. L. Kung, "Phytoconstituent-Derived Zingerone Nanoparticles Disrupt the Cell Adhesion Mechanism and Suppress Cell Motility in Melanoma B16F10 Cells," *Journal of Biotechnology* 392 (2024): 48–58, https://doi.org/10.1016/j.jbiotec.2024.06.015.

29. J. H. Park, Y. J. Shin, T. R. Riew, and M. Y. Lee, "The Indolinone MAZ51 Induces Cell Rounding and G2/M Cell Cycle Arrest in Glioma Cells Without the Inhibition of VEGFR-3 Phosphorylation: Involvement of the RhoA and Akt/GSK3β Signaling Pathways," *PLoS One* 9, no. 9 (2014): e109055, https://doi.org/10.1371/journal.pone.0109055.

30. Y. N. Hlophe and A. M. Joubert, "Vascular Endothelial Growth Factor-C in Activating Vascular Endothelial Growth Factor Receptor-3 and Chemokine Receptor-4 in Melanoma Adhesion," *Journal of Cellular and Molecular Medicine* 26, no. 23 (2022): 5743–5754, https://doi.org/10.1111/jcmm.17571.

31. M.-L. Kung, S.-T. Huang, K.-W. Tsai, T.-H. Chu, and S. Hsieh, "Nanosized Zingerone-Triggered Anti-Angiogenesis Contributes to Tumor Suppression in Human Hepatocellular Carcinoma," *Colloids and Surfaces A: Physicochemical and Engineering Aspects* 658 (2023): 130697.

32. W. J. Chan, J. Adiwidjaja, A. J. McLachlan, A. V. Boddy, and J. E. Harnett, "Interactions Between Natural Products and Cancer Treatments: Underlying Mechanisms and Clinical Importance," *Cancer Chemotherapy and Pharmacology* 91, no. 2 (2023): 103–119, https://doi.org/10.1007/s00280-023-04504-z.

33. Z. Xu, "Inhibitory Effects of Zingerone Combined With Sorafenib on Migration and Invasion of Human Liver Cancer HepG2 Cells," *Journal of Jilin University (Medicine Edition)* 45 (2019): 228–233.

34. X. Cao, C. W. Chen, K. Yin, et al., "Zingerone Facilitates Apoptosis in Triple Negative Breast Cancer Cells by Inducing Autophagy," *Journal of Biochemical and Molecular Toxicology* 38, no. 12 (2024): e70074, https://doi.org/10.1002/jbt.70074.